Conference on Modelling Fluid Flow (CMFF'15)
The 16th International Conference on Fluid Flow Technologies
Budapest, Hungary, September 1-4, 2015

CASE-SPECIFIC SEMI-EMPIRICAL GUIDELINES FOR SIMULTANEOUS REDUCTION OF LOSS AND EMITTED NOISE IN AN AXIAL FLOW FAN

Tamás BENEDEK[1], János VAD[2]

[1] Corresponding Author. Department of Fluid Mechanics, Faculty of Mechanical Engineering, Budapest University of Technology and Economics. Bertalan Lajos u. 4 – 6, H-1111 Budapest, Hungary. Tel.: +36 1 463 2464, Fax: +36 1 463 3464, E-mail: benedek@ara.bme.hu
[2] Department of Fluid Mechanics, Faculty of Mechanical Engineering, Budapest University of Technology and Economics. E-mail: vad@ara.bme.hu

ABSTRACT

The paper presents the semi-empirical investigation on the effect of the inlet axial velocity profile on the total efficiency and the upstream-radiated noise of an industrial axial flow fan rotor, installed in a free-inlet, free-exhaust setup. As a preliminary empirical diagnostics step, the emitted noise of the fan was measured by means of a Phased Array Microphone system, and the inlet axial velocity profile was taken with use of a vane anemometer. Supported by the measurements, the spanwise distribution of the emitted noise was estimated on the basis of the momentum thickness of the blade suction side boundary layer, being considered also as a loss indicator of the fan blading. The spanwise distribution of the momentum thickness was calculated with use of 2D empirical cascade correlations. The appropriateness of the applied rotor through-flow model was assessed by means of CFD simulation. Based on the semi-empirical model, the paper presents the method for surveying the dependence of the total efficiency and average sound pressure level for various inlet axial velocity profiles. Such method forms a basis for simultaneously reducing the loss and the emitted noise, while retaining the global aerodynamic performance of the fan.

Keywords: axial flow fan, efficiency, inlet velocity profile, noise, phased array microphone

NOMENCLATURE

A	[dB]	parameter in Eq. 4
d_t	[mm]	tip diameter
k	[-]	exponent in Eq. 5
L_P	[dB]	area-averaged SPL
$L_{P\Theta^*}$	[dB]	Θ^*-based approximation of SPL
L_{Θ^*}	[dB]	momentum thickness level
n	[RPM]	rotor speed
P	[Pa]	sound pressure
R	[-]	dimensionless radius
α	[°]	flow angle (from axial direction)
Φ	[-]	global flow coefficient
φ	[-]	local axial flow coefficient
η_t	[-]	total efficiency
ν	[-]	hub to tip ratio
ψ_{is}	[-]	local isentropic total pressure rise coefficient
ψ'_{sw}	[-]	local swirl loss coefficient
Θ^*	[-]	momentum thickness parameter
ω	[-]	local friction loss coefficient

Subscripts

1	rotor inlet
2	rotor outlet

Abbreviations

CFD	Computational Fluid Dynamics
PAM	Phased Array Microphone
ROSI	Rotating Source Identifier
SPL	sound pressure level
SST	Shear Stress Transport
2D	two-dimensional

1. INTRODUCTION

The inlet condition of an axial flow fan installed in an industrial environment often differs from the condition assumed in fan design or realized during the laboratory measurements forming the basis of fan catalogue data. The alteration in the inlet velocity profile influences the flow incidence to the blades, and has a major effect on the development of the boundary layer on the suction side of the fan blades. As noted in [1], the suction side boundary layer plays a key role in the generation of the aerodynamic loss over the blade surface. The boundary layer thickness can be used

as an indicator of total pressure loss [2]. The suction side boundary layer is also one of the major aero-acoustic noise sources of the fan [3]. As reported in [4], the emitted noise relates to the boundary layer thickness. These findings can be summarized as follows. a) The inlet axial velocity profile substantially influences the condition of the blade boundary layer, *via* the angle of flow incidence to the blade sections. b) As such, it has a significant effect on the aerodynamic performance and noise of the fan. c) While retaining the global aerodynamic performance of the fan (flow rate, total pressure rise), the inlet axial velocity profile may be suitably tuned for simultaneously reducing the emitted noise and the total pressure loss (i.e. improving the total efficiency). Tuning the inlet axial velocity can be carried out by means of aerodynamically profiled rotor entry sections. For example, the ISO standard [5] prescribes the use of a bellmouth entry upstream of the fan in certain measurement installations – regardless of what type of inlet condition was assumed in the design of the rotor under consideration. The bellmouth entry aims at ensuring that the flow is uniform over the entire rotor intake section. Therefore, it is a means for realizing the "uniform axial inlet condition", often used in axial fan design as an idealized condition.

In the papers [6-8], Benedek and Vad presented a diagnostics method for discovering case-specific semi-empirical correlations between the spatial distribution of the aerodynamic properties and the noise sources of the fan blading. The diagnostic method, adaptable to on-site studies of industrial fans, is based on the following experimentation: a) measurement of the rotor inlet axial velocity profile, b) Phased Array Microphone (PAM) experiments. For the case study in [7-8], it was reported that the emitted sound pressure is proportional to the momentum thickness of the blade wake in the third-octave frequency bands that are the most important from the viewpoint of human audition.

In the present paper, the evaluation method related to the case study detailed in [7-8] is further developed, enabling the case-specific semi-empirical investigation on the effect of the inlet axial velocity profile on the aerodynamic loss and the emitted noise.

This paper is considered as a Technical note for the Workshop "Beamforming for Turbomachinery Applications" organized at CMFF'15. The paper aims at provoking a discussion on the topics outlined in the Summary.

2. THE FAN OF CASE STUDY, MEASUREMENT SETUP

The fan of case study is a ventilating fan with tip diameter d_t = 300 *mm*, hub-to-tip ratio v = 0.3, tip clearance 6.6% relative to the span, and n = 1430 *RPM* rotor speed. The fan has 5 forward skewed blades and has no guide vanes. The fan was built in a short duct, in a free-inlet, free-exhaust setup (zero static pressure rise). The fan is equipped with a short, rounded inlet rim (photograph in [6]).

The inlet axial velocity profile was measured with use of a vane anemometer along two diameters being perpendicular to each other. The PAM measurement was performed from the upstream direction with use of an OptiNav Inc. Array24 microphone array. The distance between the PAM and the fan was 1.83 d_t, the PAM plate was set perpendicular to the axis of rotation, and the centre of the array coincided with the rotor axis. A more detailed description of the fan, the measurements and their evaluation can be found in [7-8].

3. SEMI-EMPIRICAL CALCULATION OF THE RADIAL DISTRIBUTION OF THE AERODYNAMIC PROPERTIES

3.1 The "simplified" through-flow model

In the papers [6-8], the aerodynamic properties were calculated along the span from the measured inlet axial velocity profile and from the geometrical data of the blading, using a two-dimensional (2D) cascade approach. In the aforementioned papers, the authors used the straightforward through-flow model inspired by reference [3] that the radial velocity component is *fully neglected* inside the rotor, i.e. the circumferentially averaged inlet and outlet axial velocity profiles are identical. This through-flow model is labelled herein as "***simplified" model***.

The "simplified" model enables the easiest treatment of through-flow in rotor analysis, and is directly consistent with the 2D cascade approach. Furthermore, it enables that the realistic angles of flow incidence to the blade sections are considered in the rotor analysis, determined directly from the measurement of the inlet axial velocity profile. Its obvious limitation is the inability to represent *any* rearrangement of the axial velocity profile through the rotor.

In the present paper, the "simplified" model is competed with a more sophisticated through-flow model, labelled herein as "***radial equilibrium" model***, and outlined in what follows.

3.2 The "radial equilibrium" model

In the case of axial flow rotors, the well-known radial equilibrium equation makes a connection between the outlet axial velocity profile and the radial distribution of total pressure rise of the blading. For further details, e.g. [3] is referred to. The dimensionless form of the radial equilibrium equation is the following:

$$\left(\eta_t - \frac{\psi_{is}(R)}{2\cdot R^2}\right)\frac{d}{dR}\psi_{is}(R) = \frac{d}{dR}\varphi_2^2(R) \qquad (1)$$

The equation was implemented in the former calculation method [6] *via* an iteration algorithm. In the first step, the radial distributions of the aerodynamic properties were computed with use of the inlet axial velocity profile. Then, the outlet axial velocity profile was recalculated from the resulting isentropic pressure rise distribution using the continuity equation, and the radial equilibrium equation (1). In the following steps, the aerodynamic properties were calculated with the *average* of the inlet and the new outlet axial velocity profiles, to be consistent with the 2D cascade approach. The computation was continued until the relative difference between the outlet axial velocities derived from the last two iteration steps stayed below 1%.

The benefit of the "radial equilibrium" model is some (restricted) capability to represent the rearrangement of the axial velocity profile through the rotor, being of significance in certain axial fans. Its main limitations are as follows. a) By principle, the radial equilibrium equation is strictly valid only farther away from the blade row. Therefore, its applicability is theoretically doubtful for a short-ducted fan, such as the one in the present case study. b) The model allows for the presence of minor radial flow velocities, associated with the rearrangement of the axial velocity profile through the rotor. However, the radial velocity is neglected in Eq. (1). c) The annulus wall boundary layers are neglected further on, such as in the "Simplified" model. d) To be consistent with the 2D cascade analysis, an obligate modelling step is the averaging of the inlet and outlet axial velocity profiles. This tends to introduce unrealistic angles of flow incidence to the blade sections, being unfavourable in predicting the aerodynamic as well as acoustic behaviour of the rotor, especially near the leading edge. For example, flow separation may be presumed near the leading-edge – due to an erroneously predicted, extreme incidence angle –, that does not occur in reality.

A judgement is to be made whether the "simplified" or the "radial equilibrium" through-flow model is more realistic in the case study under discussion. As a reference case, approximating the realistic aerodynamic behaviour of the rotor, a Computational Fluid Dynamics (CFD) simulation was carried out.

3.3 CFD technique

A steady state CFD simulation was carried out for the fan with use of the Ansys FLUENT 15 software. In the model, the supporting struts were neglected, as a reasonable modelling simplification (in preliminary studies, the aerodynamic effect of the narrow downstream struts was found negligible). With this simplification, the geometry became rotationally periodic. Therefore, only one blade passage was modelled. The computational domain was distributed to three parts: the inlet and the outlet zones were steady, and the middle zone (the short duct including the rotor) was considered as a rotating zone. During the calculations, the frozen rotor method was used. The size of the inlet and the outlet zones was 5 times the rotor radius both in the axial and radial direction. On the inlet and outlet boundaries, identical and constant pressure was prescribed, according to the measurement setup. The turbulent phenomena were modelled with use of Menter's Shear Stress Transport (SST) model [9], which is widely used in the CFD simulations of turbomachinery [10-13]. The numerical mesh was a fully structured hexamesh, containing ~2.5 million elements in such a way that two-thirds of the cells were in the rotating zone. The appropriateness of the spatial resolution of the numerical mesh was checked with a grid sensitivity study.

Corresponding to the limitations in the aerodynamic measurement data available for the industrial fan setup, the validation of the CFD technique was confined to comparing the computational results with the following measurement-based data. a) The flow coefficient, Φ, representing globally the aerodynamic operation of the elemental rotor blade cascades. b) The inlet axial velocity profile, playing a key role in tailoring the aerodynamic as well as acoustic behaviour of the individual blade cascades along the radius [8][14-15].

The Φ data derived a) from preliminary fan performance curve measurements, b) from the vane anemometer measurements on the inlet axial velocity profile, and c) from CFD modelling as an output, are presented in **Table 1**. The CFD-based global flow coefficient is in good agreement with the experimental data. The discrepancy between the CFD- and measurement-based data is within the estimated range of experimental uncertainty of ± 4 % [6]. Therefore, it is concluded that the simulation accurately represents the aerodynamic co-operation of the individual rotor blade sections.

Table 1. The global flow coefficient for 0 *Pa* static pressure rise

	Φ
Performance curve meas.	0.313
Inlet axial velocity profile meas.	0.316
CFD	0.307

The inlet axial velocity profiles, measured by means of the vane anemometer, as well as those derived from the CFD computation, are presented in **Figure 1**. The measurement uncertainty is indicated using error bars. As demonstrated in the figure, the computation fairly well resolves the spanwise gradient of the inlet axial velocity (inlet axial velocity increasing along the radius), being of significance in developing the non-free vortex

behaviour of the rotor [6]. The agreement between the computed and measured inlet axial velocity data is fair farther away from the annulus walls, i.e. in the spanwise region of R = 0.45÷0.85. Therefore, it is concluded that the simulation represents well the inlet condition of the individual blade sections in this region.

Based on the above, the CFD technique outlined herein is considered as a validated tool for representing the realistic behaviour of the rotor blade sections, with special regard to the spanwise region of R = 0.45÷0.85.

As Fig. 1 shows at R > 0.85, the simulation overpredicts the velocity deficit dedicated to flow separation anticipated at the periphery of the fan inlet section. As qualitative (wool tuft) experiments confirmed, the separation zone is considerably smaller than that predicted by the simulation.

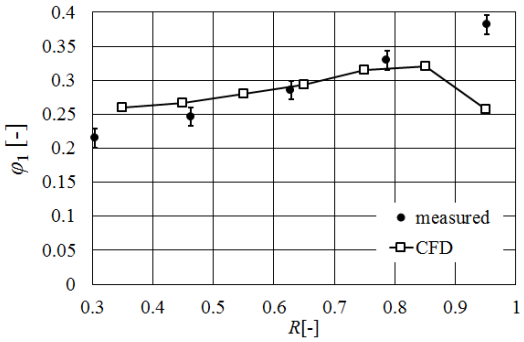

Figure 1. Inlet axial velocity profiles

3.4 Comparison between the through-flow models

In the classical 2D cascade analysis incorporated in the diagnostics method in [6-8], the inlet and outlet flow angles play a key role. In [7-8], the authors presented the correlation between the momentum thickness and the circumferentially averaged sound pressure. The wake momentum thickness is calculated in a 2D cascade approach, with use of the Lieblein diffusion factor [1], being the function of the inlet and outlet flow angles.

Therefore, the inlet and outlet flow angles are considered herein as the key indicators in investigating the appropriateness of the "simplified" and the "radial equilibrium" through-flow models.

Figures 2 to 3 present the spanwise distribution of the inlet and outlet flow angles, respectively, obtained with use of the "simplified" as well as the "radial equilibirum" model, in comparison with the CFD-based data. The semi-empirically modelled distributions obtained with use of the various through-flow models are equipped with error bars. These error bars represent the propagation of the measurement error of the axial inlet velocity – indicated in Fig. 1 –, as well as propagation of the measurement error of data on the blade geometry, in the semi-empirically modelled results.

Fig. 2 demonstrates that the "simplified" model better approximates the CFD-based inlet flow angle distribution. Taking the error bars into account, the quantitative agreement is fair in the region of R = 0.45÷0.85. The "radial equilibrium" model does not provide such a quantitative agreement over the entire region R = 0.45÷0.85.

As suggested by Fig. 3, the "radial equilibrium" model provides a better agreement with the CFD-based outlet flow angles away from the endwalls. However, investigating the region R = 0.45÷0.85, and considering the error bars as well, it is stated that the quantitative agreement between the "simplified" model and the CFD results is still satisfactory.

Based on the above observations, the following conclusion is made. Since a *single* throughflow-model is to be chosen that fairly well represents *both* the inlet and the outlet flow angle distributions, *the "simplified" model is better for the present case study*. Therefore, the "simplified" model, already applied in references [6-8], is utilised further on.

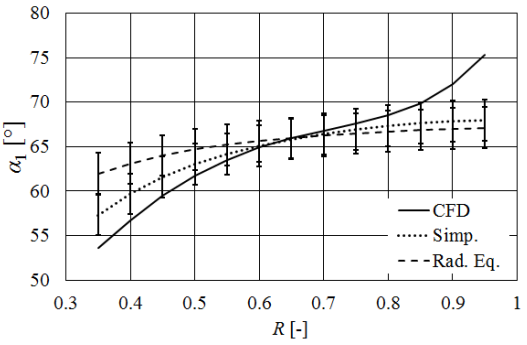

Figure 2. Inlet flow angle distributions

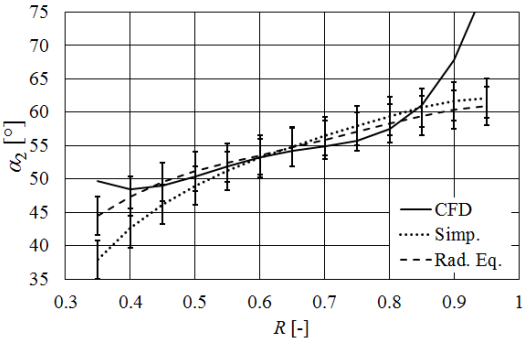

Figure 3. Outlet flow angle distributions

It is noted that a) none of the through-flow models are capable for treating the near-endwall phenomena, such as near-endwall blockage, b) the validity of the CFD tool is limited in the near-endwall region. Therefore, according to the expectations, the discrepancy between the CFD-based and semi-empirical data is increased near the annulus walls, for both the inlet (Fig. 2) and outlet (Fig. 3) flow angles.

4. CORRELATION BETWEEN THE NOISE AND THE AERODYNAMIC LOSS

The levels on a beamforming map represent the sound pressure level distribution in the investigation plane. [16] Based on that in the papers [6-8], the circumferentially averaged sound pressure level was calculated from the beamforming maps, with a third-octave band frequency resolution. At first, the noise source maps were calculated for each investigated frequency band using the Rotating Source Identifier (ROSI) [17] algorithm. Then the sound pressure values of the noise source maps in the rotor area were interpolated to an equidistant mesh. The mesh size was 100 cells both in radial and in circumferential direction. The sound pressure values were area-averaged along the circumference on this mesh, and the sound pressure level (SPL) at each radial location was calculated from the averaged sound pressure values. An example of the noise source map and the resultant SPL distribution is shown in **Figure 4**. The dashed-dotted line represents the hub radius. The circle in the upper-left corner of the map represents the estimated spatial resolution.

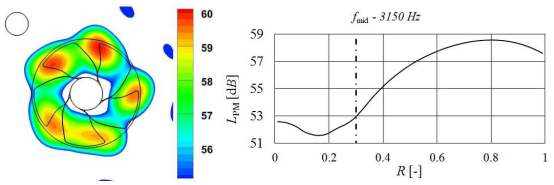

Figure 4. The noise source map, and the related averaged spanwise SPL distribution, for the frequency band of mid-frequency of 3150 *Hz*

In the papers [7] and [8], the following correlation was presented between the emitted noise and the momentum thickness of the blade wake:

$$P \propto \theta^* \tag{2}$$

By introducing the momentum thickness level

$$L_{\theta^*} = \log_{10}\left(\theta^*\right) \tag{3}$$

, the sound pressure level can be calculated using the following formula:

$$L_{P\theta^*} = A + 20 \cdot L_{\theta^*} \tag{4}$$

The spanwise distribution of the momentum thickness level is calculated. Afterwards, by best-fitting the trend functions of Eq. (4) to the PAM-based spanwise SPL distributions, the *A* values can be estimated for every third-octave bands for which the suction side boundary layer is the dominant noise source. In the present case, the third-octave bands of middle frequencies of 2000, 2500 and 3150 [*Hz*] were found as such frequency intervals. The *A* values for these frequency bands are presented in **Table 2**.

Table 2. The estimated *A* parameters

f_{mid} [*Hz*]	*A* [d*B*]
2000	106.3
2500	105
3150	98.2

5. EFFECT OF THE INLET VELOCITY PROFILE ON THE LOSS AND THE NOISE

The alteration of the inlet axial velocity profile modifies the aerodynamic behaviour of the individual blade sections. This is manifested in the alteration of the spanwise distribution of the momentum thickness. This represents the alteration of the global total pressure loss, and, *via* the trend in relationship (2), the alteration of the emitted noise as well.

In the following investigation, the global operational point of the fan is kept constant. This operating point, valid for the previous studies [6-8] as well, is characterised as follows. a) The flow rate, representing the user demand, is prescribed at $\Phi = 0.316$. b) The static pressure rise is zero (free-inlet, free-exhaust). c) The useful total pressure rise is the dynamic pressure calculated with the mean axial velocity corresponding to the constant Φ.

It is investigated herein how the modification of the inlet axial velocity profile influences the global loss and noise of the fan. Since the operational point is prescribed, only *moderate changes* are assumed in the aerodynamic as well as acoustic behaviour of the individual blade sections. In mathematical sense, such *moderate changes* allow for the following assumptions. a) For each frequency band, the proportionality represented by the relationship (2) is valid further on, with unchanged factors of proportionality (linearization for moderate changes). b) This means that the *A* values presented in Table 2 are to be used further on in predicting the sound pressure level for the various bands *Via* Eq. (4), for altered momentum thickness values.

The inlet axial velocity profile is prescribed approximately as a power function of the radius:

$$\varphi_1(R) = \varphi_1(\nu)\left(\frac{R}{\nu}\right)^k \tag{5}$$

The shape of the velocity profile is tuned by modifying the value of the *k* exponent. The axial velocity at the hub, represented by $\varphi_1(\nu)$ in Eq. (5), is set in accordance with the integral condition of the prescribed Φ value.

As already noted, the "simplified" through-flow model was applied in the study reported below. The

global total efficiency and the average sound pressure level were investigated as functions of k for the interval $k = 0 \div 1$, as demonstrated in **Figures 5 to 6**. $k = 0$ and $k = 1$ represent a uniform axial inlet condition, and a spanwise linearly increasing inlet axial velocity, respectively.

The global total efficiency (Fig. 5) is the mass-average of the local total efficiency over the span. The local total efficiency was calculated as presented in Eq. (6). It considers the blade friction loss (ω), calculated from the momentum thickness [1]; and the swirl loss (ψ'_{sw}), being equal to the mass-averaged dynamic pressure corresponding to the outlet swirl velocity.

$$\eta_t = \frac{\psi_{is} - \omega - \psi'_{sw}}{\psi_{is}} \qquad (6)$$

The average sound pressure level (Fig. 6) was calculated as follows. The spanwise-resolved sound pressure distributions were estimated using the Eq. (4). Then the sound pressure values were area-averaged over the annulus area for the individual frequency bands. The resultant average sound pressure has been presented in a logarithmic level form in Fig. 6.

The measured inlet velocity profile, presented in Fig. 1, and corresponding to the studies carried out so far [6-8], can be approximated using Eq. (5) with a substitution of $k = 0.45$. The results corresponding to this exponent – in what follows, referred to as "measured case" – are indicated in Figs 5 to 6 using dashed lines.

As Fig. 5 shows, the total efficiency increases with k. The main reason is the moderation of the swirl loss, being the dominant loss in Eq. (6), with increasing k values. With reference to the measured case, an efficiency deterioration of 1 % and an efficiency gain of 0.7% are predicted at $k = 0$ and $k = 1$, respectively.

In the literature [18], the classic formula by Regenscheit is proposed for estimating the emitted noise of the fan from the global aerodynamic properties. Considering that the global operational point is fixed in the present case study, the alteration of global efficiency, according to Fig. 5, is the only factor that influences the noise emission *via* the formula in [18]. Considering the efficiency deterioration of 1 %, the formula in [18] predicts an increase of noise of only ≈ 0.4 dB for the $k = 0$ case, relative to the measured case. This prediction is optimistic, in comparison with the results in Fig. 6, as discussed below.

The average SPL in Fig. 6 reaches its minimum at $k = 0.6$, being close to the measured case. The maximum SPL value can be found at $k = 0$, for which the increase of noise is ≈ 2 dB compared to the measured case – more than predicted on the basis of [18].

The above observations suggest that the fan in this case study exhibits favourable aerodynamic and acoustic features when the measured non-uniform axial inlet velocity profile ($k = 0.45$) is realized. The efficiency is at the middle of the investigated efficiency range of 81 ± 1 %, and the emitted noise is practically at the minimum.

Equipping the fan with an aerodynamically designed bellmouth entry, as proposed in [5], would approximate the uniform axial inlet condition of $k = 0$. Contrary to the expectations, the bellmouth entry is predicted herein to deteriorate the total efficiency by 1 %, and to increase the boundary layer related noise by 2 dB. These undesired changes are minor from a quantitative point of view, but draw the attention to the unwanted tendencies that may be more significant in other cases. The "myth" that the bellmouth entry contributes to the minimization of loss – and, as such, to the minimization of noise [18] – is to be replaced by a more systematic, tuned design of the rotor + its inlet section, for simultaneous reduction of loss and noise.

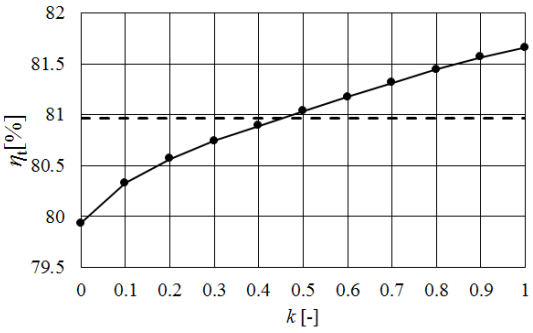

Figure 5. The total efficiency as a function of k

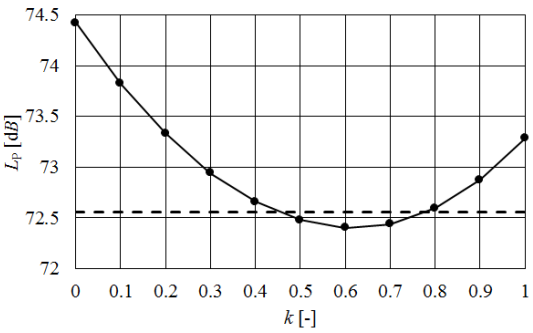

Figure 6. The average SPL as a function of k

CONCLUSION AND FUTURE REMARKS

In the paper, as continuation of research reported in [6-8], the effect of the inlet axial velocity profile on the total efficiency and on the upstream-radiated noise of an axial flow fan have been investigated, by means of a concerted aerodynamic-acoustic diagnostics method, incorporating PAM measurements. The results are

summarized as follows, and some remarks are made for the continuation of the research programme.

1) The appropriateness of the "simplified" and the "radial equilibrium" through-flow models was investigated by comparing the modelled inlet and outlet flow angle distributions to computational results obtained by means of an experimentally validated CFD tool. In the present study, the "simplified" model, prescribing identical rotor-inlet and -outlet axial velocity profiles, was judged as being more realistic than the "radial equilibrium" model. Therefore, the "simplified" model has been used in the present case study. One important, generally valid advantage of the "simplified" model is that the realistic angles of flow incidence to the blade sections are considered in the rotor analysis, determined directly from the measurement of the inlet axial velocity profile. The proper modelling of inlet flow angles is essential in the concerted aerodynamic-acoustic analysis.

2) Based on semi-empirical correlations obtained in the previous research steps, a methodology was elaborated for a systematic investigation of the effect of the altered inlet velocity profile on the global total efficiency and the upstream-radiated average SPL. The inlet axial velocity profile was modelled by means of a power function, and the shape of the velocity profile was controlled by means of altering the power exponent k. Cases extending from the uniform axial inlet condition (k = 0) to spanwise linearly increasing axial inlet velocity (k = 1) were studied.

3) It has been found that the measured non-uniform inlet axial velocity profile provides a favourable aerodynamic and acoustic operation for the fan: the efficiency is at the middle of the investigated efficiency range of 81 ± 1 %, and the emitted noise is practically at the minimum.

4) Equipping the fan with an aerodynamically designed bellmouth entry would approximate the uniform axial inlet condition of k = 0. The bellmouth entry was predicted to deteriorate the total efficiency by 1 %, and to increase the emitted noise by 2 dB. This underlines the importance of systematic, tuned design of the rotor + its inlet section, for simultaneous reduction of loss and noise.

5) In the future, the predictions are to be confirmed by experiments. For this purpose, a bellmouth entry is to be designed and manufactured for realization of uniform axial velocity profile. The bellmouth entry is to be installed to the inlet of the case study fan, instead of the presently available short, rounded inlet rim. The aerodynamic and acoustic measurements are to be repeated for confirmation of the trends outlined in the previous point.

ACKNOWLEDGEMENTS

This work has been supported by the Hungarian National Fund for Science and Research under contract No. OTKA K 112277.

Gratitude is expressed to Ms. Anna Ilona Sipos for her help in programing, to Ms. Anna Tóth for the CFD simulations, and to Dr. Csaba Horváth and Mr. Bence Tóth for their useful comments.

The work relates to the scientific programs "Development of quality-oriented and harmonized R+D+I strategy and the functional model at BME" (Project ID: TÁMOP-4.2.1/B-09/1/KMR-2010-0002) and "Talent care and cultivation in the scientific workshops of BME" (Project ID: TÁMOP-4.2.2/B-10/1-2010-0009).

REFERENCES

[1] Vad, J., 2011, "Correlation of Flow Path Length to Total Pressure Loss in Diffuser Flows", *Proceedings IMechE, Part A - J Power Energy*, Vol. 225, pp. 481-496.

[2] Lieblein, S., 1965, *Experimental Flow in Two-Dimensional Cascades, Chapter VI in Aerodynamic Design of Axial-Flow Compressors*, NASA SP-36, Washington D.C.

[3] Carolus, T., 2003, *Ventilatoren,* Teubner Verlag.

[4] De Gennaro, M., and Kuehnelt, H., 2012, "Broadband Noise Modelling and Prediction for Axial Fans," Proc. *International Conference on Fan Noise, Technology and Numerical Methods (FAN2012)*, Senlis, France, ISBN 978-0-9572374-1-4.

[5] EN ISO 5801:2008 (E), "*Industrial Fans. Performance testing using standardized airways*".

[6] Benedek, T., and Vad, J., 2014, "Concerted Aerodynamic and Acoustic Diagnostics of an Axial Flow Industrial Fan, Involving the Phased Array Microphone Technique," *ASME Paper* GT2014-25916.

[7] Benedek, T., and Vad, J., 2015, "Spatially Resolved Acoustic and Aerodynamic Studies Upstream and Downstream of an Industrial Axial Fan with Involvement of the Phased Array Microphone Technique," Proc. *11th European Conference on Turbomachinery Fluid Dynamics and Thermodynamics*, Madrid, Spain, Paper # 128.

[8] Benedek T., and Vad J., 2015, "An industrial on-site methodology for combined acoustic-aerodynamic diagnostics of axial fans, involving the Phased Array Microphone technique", *Int. J Aeroacoustics* (accepted)

[9] Menter, F.-R., 1993, “Zonal two equations k–ω turbulence models for aerodynamic flows”, AIAA paper 93-2906.

[10] Reese, H., Carolus, T., and Kato, C., 2007, “Numerical prediction of the aeroacoustic sound sources in a low pressure fan with inflow distortion”, Proc. *International Conference on Fan Noise, Technology and Numerical Methods (FAN2007)*, Lyon, France.

[11] Younsi, M., Bakir, F., Kouidri, S., and Rey, R., 2007, “Numerical and experimental study of unsteady flow in a centrifugal fan”, *Proceedings IMechE, Part A - J Power Energy*, Vol. 221, pp. 1025-1036.

[12] Bamberger, K., and Carolus, T., 2012, “Optimization of axial fans with highly swept blades with respect to losses and noise reduction”, Proc. *International Conference on Fan Noise, Technology and Numerical Methods (FAN2012)*, Senlis, France.

[13] Guédeney, T., and Moreau, S., 2015, “Unsteady RANS simulations of a low speed fan for analytical tonal noise prediction”, Proc. *11th European Conference on Turbomachinery Fluid Dynamics and Thermodynamics*, Madrid, Spain, Paper # 123.

[14] Sharland, I. J., 1964, “Sources of noise in axial flow fans”, *J Sound Vib*, Vol. 3, pp. 302-322.

[15] Carolus, T., Schneider, M., and Reese, H., 2007, “Axial fan broadband noise and prediction”, *J Sound Vib*, Vol. 300, pp. 50-70.

[16] Koop, L., 2006, “Beamforming Methods in Microphone Array Measurements: Theory, Practice and Limitations,” *VKI Lecture Series 2007/01: Experimental Aeroacoustics*, Rhode Saint-Genése, Belgium

[17] Sijtsma, P., Oerlemans, S., and Holthusen, H., 2001, “Location of Rotating Sources by Phased Array Measurements”, AIAA Paper 2001-2167.

[18] VDI 3731 Blatt 2, 1990, “*Emissionkennwerte technischer Schallquellen. Ventilatoren.”*